Moonlighting function of Phytochelatin synthase 1 in extracellular defense against fungal pathogens

Kian Hematy[a,b,1,*], Melisa Lim[a,b,*], Candice Cherk[b], Mariola Piślewska-Bednarek[c,d], Clara Sanchez-Rodriguez[e2], Monica Stein[a3], Rene Fuchs[f4], Christine Klapprodt[f], Volker Lipka[f], Antonio Molina[e,g], Erwin Grill[h], Paul Schulze-Lefert[c], Paweł Bednarek[c,d,5], Shauna Somerville[a,b,5]

[a] Carnegie Institution for Science, Department of Plant Biology, 260 Panama Street, Stanford, CA 94350, USA

[b] Energy Biosciences Institute, 130 Calvin Hall, Mail Code 5230, University of California at Berkeley, Berkeley, CA 94720, USA

[c] Department of Plant Microbe Interactions, Max Planck Institute for Plant Breeding Research, Carl-von-Linné-Weg 10, D-50829 Köln, Germany

[d] Institute of Bioorganic Chemistry, Polish Academy of Sciences, Noskowskiego 12/14, 61-704 Poznań, Poland

[e] Centro de Biotecnología y Genómica de Plantas, Universidad Politécnica de Madrid - Instituto Nacional de Investigación y Tecnología Agraria y Alimentaria (INIA), Campus de Montegancedo-UPM, E-28223-Pozuelo de Alarcón (Madrid), Spain

[f] University of Goettingen, Schwann-Schleiden Research Center for Molecular Cell Biology, Albrecht-von-Haller-Institute for Plant Sciences, Department of Plant Cell Biology, Julia-Lermontowa-Weg 3, D-37077 Goettingen, Germany

[g] Departamento de Biotecnología-Biología Vegetal, Escuela Técnica Superior de Ingeniería Agronómica, Alimentaria y de Biosistemas, E-28020-Madrid, Spain

[h] Lehrstuhl für Botanik, Technische Universtät München, D-85350 Freising, Germany

[*] KH and ML contributed equally to this work.

[1] Present address: Institut Jean-Pierre Bourgin, INRA, AgroParisTech, CNRS, Université Paris-Saclay, Versailles, France.

[2] Present address: Department of Biology, ETH Zurich, 8092 Zurich, Switzerland

[3] Present address: University of the Valley Guatemala, Guatemala City 01015, Guatemala

[4] Present address: Staatliches Weinbauinstitut Freiburg, Merzhauser Straße 119, D-79100 Freiburg im Breisgau, Germany

[5]To whom correspondence should be addressed. E-mail: ssomerville@berkeley.edu, bednarek@ibch.poznan.pl

One-Sentence Summary :

PCS1 is a moonlighting protein, which in addition to its function in abiotic stress response is indispensable for proper extracellular immune responses and pathogen-triggered glucosinolate metabolism.

Author Contributions

KH, ML, VL, AM, EG, PSL and SS designed the research, KH, ML, CC, PB, MPB, CSR, MS, RF, CK performed research and analyzed data. KH and SS wrote the manuscript with contributions from PB, VL and PSL.

ABSTRACT

Phytochelatin synthase (PCS) is a key component of heavy metal detoxification in plants. PCS catalyzes both the synthesis of the peptide phytochelatin from glutathione as well as the degradation of glutathione conjugates via peptidase activity. Here, we describe a role for PCS in disease resistance against plant pathogenic fungi. The *pen4* mutant, which is allelic to *cadmium insensitive 1* (*cad1/pcs1*) mutants, was recovered from a screen for Arabidopsis mutants with reduced resistance to the non-adapted barley fungal pathogen, *Blumeria graminis* f. sp. *hordei*. PCS1, which is found in the cytoplasm of cells of healthy plants, translocates upon pathogen attack and colocalizes with the PEN2 myrosinase on the surface of immobilized mitochondria. *pcs1* and *pen2* mutant plants exhibit similar metabolic defects in the accumulation of pathogen-inducible indole glucosinolate-derived compounds, suggesting that PEN2 and PCS1 act in the same metabolic pathway. The function of PCS1 in this pathway is independent of phytochelatin synthesis and deglycination of glutathione conjugates, as catalytic-site mutants of PCS1 are still functional in indole glucosinolate metabolism. In uncovering a peptidase-independent function for PCS1, we reveal this enzyme to be a moonlighting protein important for plant responses to both biotic and abiotic stresses.

INTRODUCTION

As sessile organisms, plants have developed sophisticated mechanisms that allow them to adapt to and survive the biotic and abiotic stresses that they encounter in their environments. Different stress signaling pathways are connected to maximize plant fitness (Berens et al., 2019). For instance, one evolutionary conserved mechanism involves phytohormone signaling mediated by abscisic acid, which promotes abiotic stress tolerance and suppresses signaling of the biotic stress-related phytohormone salicylic acid (Berens et al., 2017). On the other hand, an overlapping enzymatic machinery is engaged to cope with xenobiotics and pathogen stress. The metabolism of xenobiotics, including plant metal tolerance, as well as the biosynthesis of sulfur-containing immunomodulatory and antimicrobial secondary metabolites such as glucosinolates and indole-type phytoalexins involves in Brassicaceae species the formation and processing of glutathione conjugates (Grill et al., 1989; Cobbett and Goldsbrough, 2002; Bednarek et al., 2009; Pastorczyk and Bednarek, 2016; Czerniawski and Bednarek, 2018).

Invasive growth is an essential part of the pathogenesis of many fungal and oomycete plant pathogens, and extracellular defense mechanisms play a critical role in blocking their entry into plant cells (Underwood and Somerville, 2008; Hematy et al., 2009). For example, *Arabidopsis thaliana* is an inappropriate or non-host plant for the non-adapted barley powdery mildew pathogen, *Blumeria graminis sp. hordei* (*Bgh*) (Lipka et al., 2008). The ability of Arabidopsis cells to resist *Bgh* entry is partly dependent on the PENETRATION (PEN) proteins. For instance, mutants of the syntaxin PEN1 (=SYP121) (Collins et al., 2003), the myrosinase PEN2 (Lipka et al., 2005) and the ABC transporter PEN3 (=PDR8) (Stein et al., 2006) are more susceptible to *Bgh* entry and exhibit increased formation of the fungal feeding structure, the haustoria, in leaf epidermal cells. It has been shown that PEN2 hydrolyzes indole glucosinolates (IGs), a class of sulfur-containing secondary metabolites, to form products that could act as broad-spectrum toxins and confer antifungal defense in the extracellular space at pathogen contact sites (Bednarek et al., 2009). It has also been suggested that IG-derived compounds are signaling molecules for callose deposition following treatment with the microbe-associated molecular pattern (MAMP) flagellin (flg22), a peptide epitope derived from the bacterial motor protein (Clay et al., 2009). Recently, Arabidopsis Glutathione-*S*-Transferase class-tau member 13 (GSTU13) was identified as an indispensable component of the PEN2 immune pathway for IG metabolism (Piślewska-Bednarek et al., 2018), suggesting that this pathway involves conjugation of the tripeptide

glutathione (ECG) with unstable isothiocyanates (ITCs) that are products of IG metabolism and further processing of the resulting adducts to biologically active molecules. Arabidopsis PAD2/CAD2, which encodes γ-glutamylcysteine synthetase (γ-ECS) and catalyzes the first committed step of glutathione biosynthesis, is essential for biotic stress-induced accumulation of IGs and the PEN2 immune pathway (Bednarek et al., 2009). The same enzyme is also needed for heavy metal ion tolerance, as glutathione is the precursor of heavy-metal chelating polypeptides, called phytochelatins, which in Arabidopsis are predominantly produced by phytochelatin synthase 1 (PCS1) (Grill et al., 1985; Grill et al., 1989; Howden et al., 1995; Rea, 2006). Notably, *pcs1* mutants display elevated cell death responses in leaves upon inoculation with the oomycete pathogen *Phytophthora infestans*, enhanced susceptibility to the bacterial phytopathogen *Pseudomonas syringae* DC3000 and reduced callose deposition upon treatment with the peptide-epitope flg22 derived from the motor protein of *P. syringae*, indicating that apart from a function in tolerance towards heavy metal ions, PCS1 has also a role in Arabidopsis immunity (Clay et al., 2009; Kühnlenz et al., 2015; De Benedictis et al., 2018). Moreover, given that a PCS from *Caenorhabditis elegans* was able to restore phytochelatin production, but not to revert the cell death phenotype in the *pcs1* mutant background, it was suggested that PCS1 function in plant immunity is not dependent on phytochelatin accumulation (Kühnlenz et al., 2015). Finally, *pen2* and *pcs1* mutants were shown to share an aberrant pathogen-triggered accumulation and secretion of IGs and their metabolism products. This includes a hyperaccumulation of 4-methoxyindol-3-ylmethyl glucosinolate, reduced levels of indol-3-ylmethyl amine and raphanusamic acid, as well as reduced secretion of 4-methoxyindol-3-yl methanol and *S*-(4-methoxyindol-3-ylmethyl) cysteine (Matern et al., 2019).

We present here the isolation and characterization of Arabidopsis mutants with defects in a *PENETRATION* resistance gene (*PEN*) designated *PEN4*. These mutants are allelic with *pcs1* and are sensitive to invasive powdery mildew pathogens. We show that PCS1 is translocated underneath pathogen contact sites, where it co-localizes with PEN2, which is known to accumulate on the surface of immobilized mitochondria (Fuchs et al., 2016). Mutagenesis of PCS1 residues abolishing phytochelatin synthesis affects tolerance to heavy metals but does not alter PCS1 function in IG metabolism or extracellular defense. Together our results show that PCS1 acts in the PEN2 pathway and is a multi-functional protein with two independent activities. As well as its long-known function in the synthesis of the peptide phytochelatin for

136 heavy metal tolerance, PCS1 also has an independent role in IG metabolism and immune
137 responses.
138
139

RESULTS

Mutations in *PHYTOCHELATIN SYNTHASE 1* result in enhanced invasive growth of several fungal pathogens

The *pen4* mutant was isolated in a screen for Arabidopsis lines that allowed increased penetration of the non-adapted barley powdery mildew *Bgh* into leaf cells (Stein et al., 2006). Typically, 5–10% of germinated *Bgh* conidiospores successfully breach the plant cell wall and differentiate into fungal haustoria for nutrient uptake in Arabidopsis Col-0 (wild-type) leaf epidermal cells (Fig. 1A, arrowhead), while the remaining attempts at fungal entry culminate in *de novo*-synthesized callose-rich deposits called papillae (Fig. 1A, star). The frequency of haustorium formation by *Bgh* increases to 20–25% on the leaves of *pen4* plants (Fig 1C).

Map-based cloning of *PEN4* revealed that it encodes phytochelatin synthase (PCS1). PCS proteins are known for their glutathione γ-glutamylcysteinyltransferase activity (EC 2.3.2.15). The mutation in *pen4* results in a premature stop codon that truncates the protein at amino acid residue 236 (Fig. 1E) in the middle of a DUF1984 domain (PF09328), which is always associated with the phytochelatin domain (PF05023) (Rea, 2006). To confirm that the mutation in *PCS1* is responsible for enhanced *Bgh* entry into *pen4* leaves, we tested another *pcs1* allele previously isolated in screens for plants with reduced tolerance to heavy metal cadmium ions (*cad1-3*) (Howden et al., 1995) and a null line carrying a T-DNA insertion in the second exon of *PCS1* (Blum et al., 2007). All *pcs1* lines were more susceptible to *Bgh* haustorium formation than the wild type Col-0 (Fig. 1C). Like the parental lines, the F1 progeny of a cross between the *cad1-3* and *pen4* plants led to an increase of *Bgh* entry rates up to 20%, indicating that *pen4* is allelic to *cad1-3* (Fig. S1).

Consistent with an impaired function of PCS1, the *pen4* mutant also showed decreased tolerance to cadmium (Fig. 1B, D). PCS2, the second isoform of the phytochelatin synthase in Arabidopsis, shares 83% amino acid identity with PCS1. Although PCS2 can synthesize phytochelatins in response to heavy metals, the gene appears to be dispensable for heavy metal tolerance (Fig. 1D, (Blum et al., 2007). We asked whether PCS2, like PCS1, has a role in penetration resistance to fungal pathogens. A mutant line harboring a T-DNA insertion that abolishes *PCS2* expression (*pcs2*) (Blum et al., 2007) showed a frequency of cell entry by *Bgh* that was comparable to wild-type Col-0 plants (Fig. 1C). Furthermore, a line harboring T-

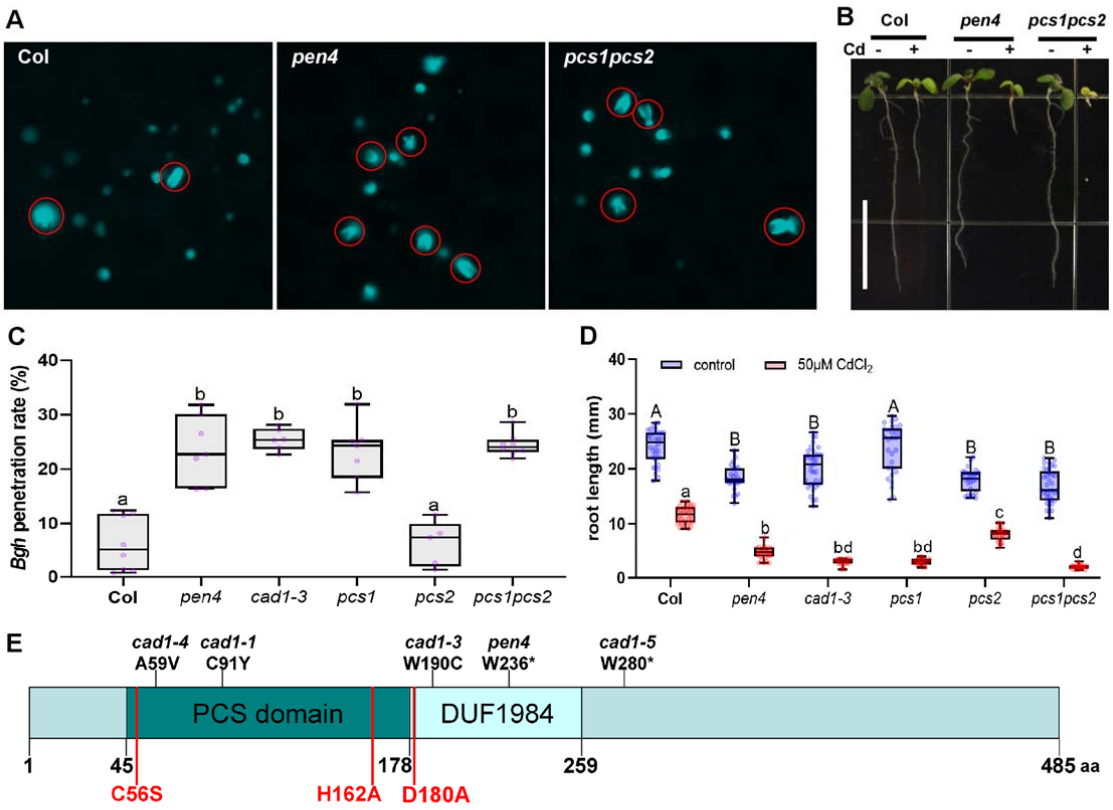

Figure 1. **PEN4/PCS1 is important for both non-host penetration resistance and heavy metal tolerance.**
(A) Aniline blue-stained leaves of 3-week-old Arabidopsis plants 24 h after inoculation with Bgh. Aniline blue stains callose papillae symptomatic of failed penetration attempts, and callose-containing encasements of haustorial necks formed after a successful penetration by the fungal appressorium (red circles). (B) 7-day-old Arabidopsis seedlings of the indicated genotype grown in the presence or absence of cadmium (50 µM CdCl2, between 25-30 individual seedlings for each genotype/treatment grown on the same plate have been used for the measurement). (C) Box plots showing penetration rate of Bgh spores on leaves of 3-week-old Arabidopsis plants. Measurements were done 24 h post-infection on the first true leaves of 5–6 individual plants (600–800 total penetration attempts counted per genotype). Whiskers represent Min-Max values. Different letters show statistical differences according to Tukey's post-hoc test following one-way ANOVA There was a significant genotype effect ($p<0.0001$). (D) Root length of 7-day-old seedlings grown in the presence or absence of cadmium (50 µM CdCl2, between 25-30 individual seedlings for each genotype/treatment grown on the same plate have been used for the measurement). Different letters show statistical differences according to Tukey's post-hoc test following two-way ANOVA. There were significant main effects for Cd treatment and genotype ($p<0.001$) and a significant interaction effect ($p<0.001$). (E) Domain organization of PCS1 showing the position of several mutant alleles (above) and residues important for phytochelatin synthesis (below in red).

174 DNA insertions in both *PCS1* and *PCS2* (*pcs1 pcs2*) (Blum et al., 2007) did not consistently
175 exhibit a higher incidence of cell entry by *Bgh* than the *pcs1* single mutant (Fig. 1C). As with
176 heavy metal tolerance, PCS2 has no detectable role in extracellular defense to the non-adapted
177 pathogen. Furthermore, impaired disease resistance of the *pen4* or *pcs1 pcs2* double mutant
178 line could be complemented by transforming these mutants with *PCS1* expressed under the
179 control of its native promoter or a 35S promoter and tagged with GFP at its N-terminus (used
180 later on in this study). Together, these data indicate that *PCS1* plays a role in limiting plant
181 cell entry by *Bgh*.
182
183 To determine whether *PCS1* is important for resistance responses to other fungal pathogens,
184 we inoculated *pen4* plants with the necrotrophic fungi *Botrytis cinerea* (Fig. S2A) and

185 *Plectosphaerella cucumerina* (Fig. S2B) (Sanchez-Rodriguez et al., 2009). Infection with
186 both fungi was more severe in these mutant plants. Furthermore, *pen4* mutants, like *pen2*
187 mutants, were hypersusceptible to *Golovinomyces cichoracearum*, a powdery mildew adapted
188 for growth on Arabidopsis (Fig. S2C). Together, these results show that PCS1 is important
189 both in preventing the entry of non-adapted pathogens and in basal defense responses against
190 multiple fungal pathogens.
191
192
193 **Translocation of cytosolic PCS1 to immobile mitochondria underneath pathogen contact**
194 **sites.**
195
196 Powdery mildew attack induces dramatic changes in cellular organization at the site of
197 attempted fungal penetration (Underwood and Somerville, 2008). Several proteins that
198 function in preventing host cell entry by *Bgh* show focal accumulation beneath fungal
199 appressoria within epidermal cells at the site of attack, suggesting that these proteins act
200 locally in extracellular defense responses (Koh et al., 2005; Underwood and Somerville,
201 2008). For instance, entry attempts of the fungus trigger local arrest of a subpopulation of
202 mitochondria underneath *Bgh* appressoria, which is accompanied by transient aggregate
203 formation of tail-anchored PEN2-GFP on the surface of these organelles (Fuchs et al., 2016).
204 The plasma membrane-resident PEN3-GFP focally accumulates as disks, sometimes with
205 bullseye-like "rings" around these contact sites (Koh et al., 2005; Stein et al., 2006).
206
207 Given PCS1's involvement in limiting host cell entry, we tested whether PCS1 localized to
208 the site of fungal attack. To this end, we generated GFP fusions at either the amino- or
209 carboxy-terminus of PCS1 under control of the 35S promoter in the *pen4* background (Fig.
210 2A-B). In addition, we generated a transgenic *pcs1 pcs2* double mutant line expressing RFP-
211 PCS1 driven by the 35S promoter. In non-inoculated leaf epidermal cells, the RFP-PCS1
212 fluorescence signal suggested a cytosolic localization similar to that of free GFP expressed
213 under the control of the 35S promoter (EGAD line; (Cutler et al., 2000); Fig. 2C). This is
214 consistent with the absence of canonical organelle targeting sequences or predicted
215 transmembrane domains in PCS1. In pathogen-challenged leaf epidermal cells, in addition to
216 their cytosolic localization, GFP-PCS1 and PCS1-GFP localized to bright round aggregates
217 underneath *Bgh* contact sites (Fig. 2A,B); GFP alone did not exhibit this localization (Fig.
218 2D), excluding the possibility that the fluorescent tag is itself driving PCS1 aggregation

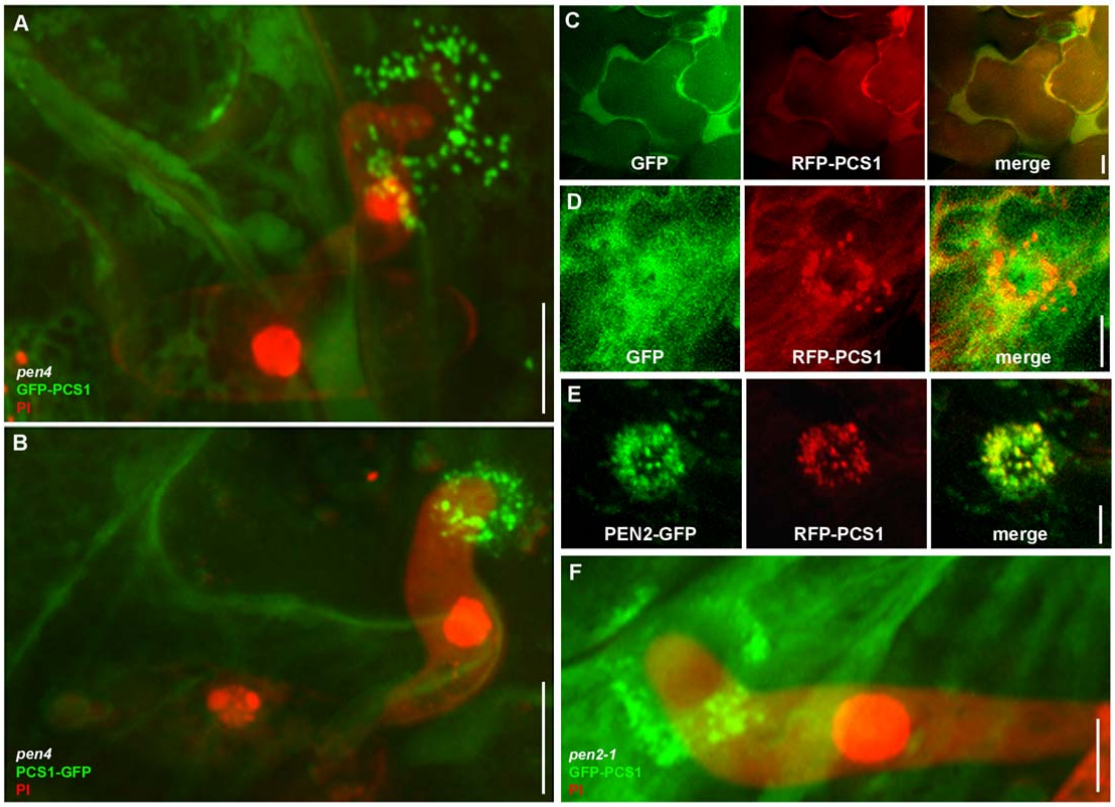

Figure 2. **Pathogen attack triggers translocation of cytoplasmic PCS1 and mitochondrial colocalization with PEN2 at fungal penetration sites.** 3-week-old Arabidopsis seedlings were inoculated with the non-adapted powdery mildew Blumeria graminis sp. hordei (Bgh). The epidermis of the first true leaves was visualized by confocal laser scanning microscopy 12–16 h after Bgh inoculation. The fungal structures are stained with propidium iodide except in GFP/RFP localization experiments. All pictures represent averaged Z-projection of stacks of 30–50 sections, except in (C) where a single median section is shown. Localization at the attempted penetration site of GFP-PCS1 (A) or PCS1-GFP (B) in a pen4 mutant leaf epidermal cell. (C) Cytosolic localization of soluble GFP with RFP-PCS1 in non-infected epidermal cells. (D) Translocation of RFP-PCS1 but not of soluble GFP into aggregates at the penetration site. (E) Colocalization of RFP-PCS1 with mitochondria-associated PEN2-GFP at the penetration site. (F) Localization of GFP-PCS1 in a pen2 mutant background after Bgh infection. Scale bar is either 10 µm (A-C) or 5 µm (D-F).

underneath pathogen contact sites. Similarly, RFP-PCS1 also accumulated focally at incipient *Bgh* entry sites (Figure 2D, E). During the early stages of fungal entry, PCS1 tightly localized just beneath the tip region of the appressorium (Fig. 2B,E), while at later stages the aggregates appeared more dispersed and excluded from the center of the penetration site (Fig. 2A,D,F). Furthermore, the signal recruiting PCS1 to attempted entry sites was able to cross cell frontiers (Fig. 2F, GFP-PCS1 from two adjacent cells organized as a ring around the fungal penetration site).

As the PCS1 aggregation pattern at pathogen contact sites was reminiscent of PEN2 localization upon *Bgh* inoculation, we examined the localization of RFP-PCS1 in PEN2-GFP-expressing transgenic plants (Lipka et al., 2005). In pathogen-free plants, RFP-PCS1 showed a strong cytoplasmic fluorescence signal, similar to the GFP-tagged version described above, whereas PEN2-GFP was detectable in the cytoplasm and in the periphery of mobile

membrane compartments (Fig. S3C-E) recently shown to represent peroxisomes and mitochondria (Fuchs et al., 2016). Pathogen challenge induced co-localization of RFP-PCS1 and PEN2-GFP in aggregate structures with enhanced fluorescence intensity (Fig. 2E). RFP-PCS1 did not translocate to all PEN2-GFP-tagged organelles surrounding attempted fungal entry sites, but was confined to a subset with increased PEN2-GFP fluorescence and aggregation (Fig. S3E). These organelles were recently identified as a subpopulation of epidermal mitochondria, which become immobile at plant-pathogen contact sites (Fuchs et al., 2016).

To investigate a possible docking role of PEN2 for PCS1, we examined PCS1 relocalization after inoculation in a *pen2-1* null mutant background (Lipka et al., 2005). Both GFP-PCS1 and RFP-PCS1 are able to aggregate underneath *Bgh* contact sites even in the absence of PEN2 (Fig. 2F, S3F), suggesting that mitochondria-associated PEN2 is not necessary for the recruitment of PCS1 to these organelles.

PCS1 catalytic residues are not required for extracellular defense

When preparing our fusion constructs to investigate the subcellular localization of PCS1 (GFP-PCS1 and PCS1-GFP), we found a striking difference that suggested the two functions of PCS1 in heavy metal tolerance and disease resistance could be uncoupled. Consistent with a previous study (Blum et al., 2010), both GFP fusions were soluble and were found to localize to the cytosol. To verify the functionality of the recombinant proteins, we tested their ability to complement the characteristic penetration resistance and cadmium tolerance defects of the *pen4* mutants. The cadmium hypersensitivity of *pen4* could be complemented by either GFP-PCS1 or PCS1-GFP fusions (Fig. 3B), which resulted in both cases in the accumulation of high levels of phytochelatin upon cadmium treatment (Fig. 3C), suggesting that both fusions are functional. However, the penetration resistance defect of *pen4* could only be complemented by the GFP-PCS1 fusion (Fig. 3A). Similar to GFP-PCS1, RFP-PCS1 was fully functional in both penetration resistance and heavy metal tolerance (Fig. S3A-B). Both GFP/RFP-PCS1 and PCS1-GFP relocalize as aggregates at focal sites of attempted fungal penetration (Fig. 2A, B), indicating that the lack of complementation of entry resistance in *pen4* by PCS1-GFP is not due to mislocalization of the PCS1-GFP fusion protein. The difference in complementation of the *pen4* disease resistance phenotype by PCS1-GFP versus GFP-PCS1 is in accordance with an earlier study of Kühnlenz et al. (2015) who showed that

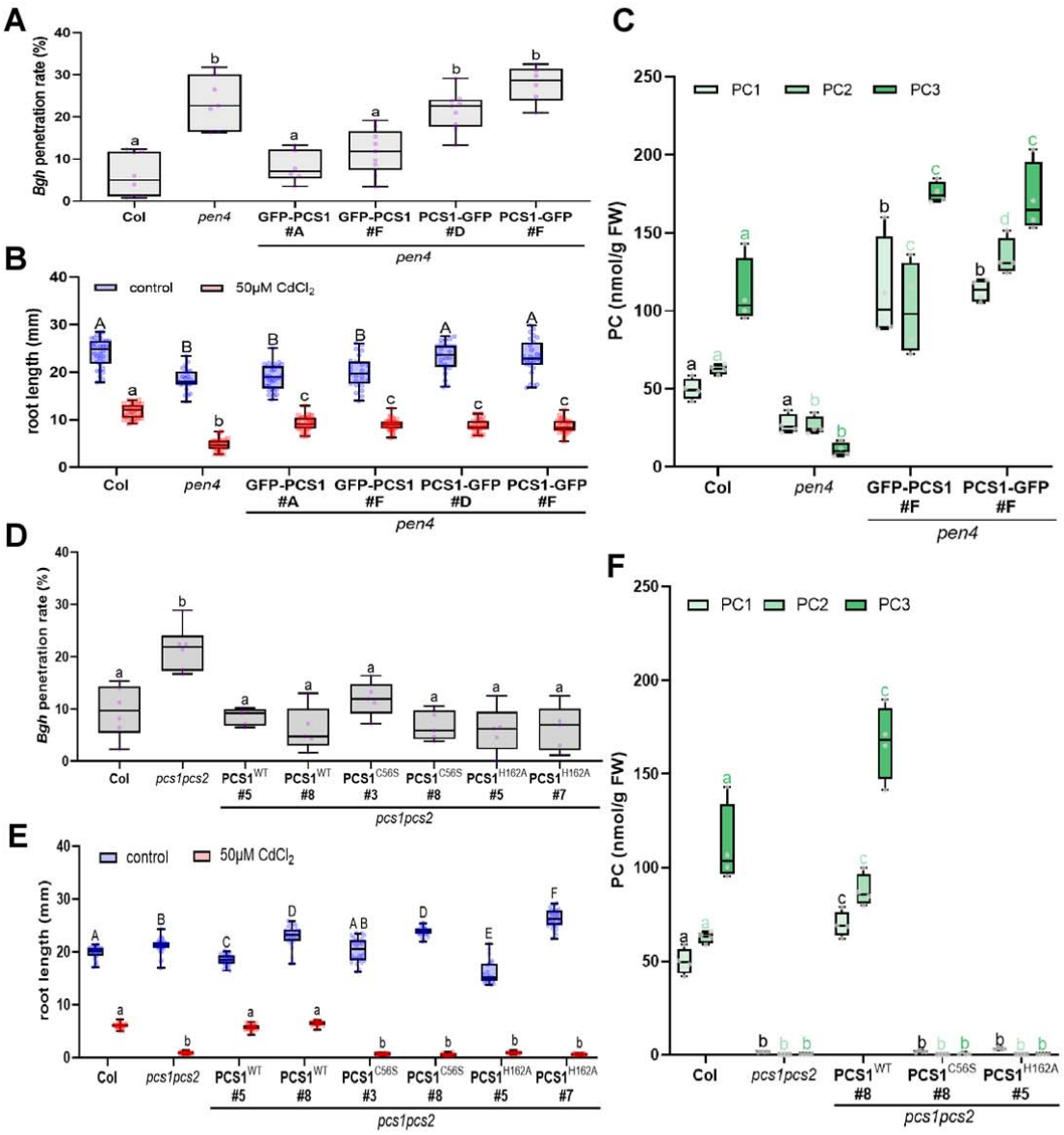

Figure 3: **Phytochelatin synthesis is required for heavy metal tolerance but not for non-host resistance.**
(A, D) Box plots showing penetration rate of Bgh spores on leaves of 3-week-old Arabidopsis plants. Measurements were done 24 h post-infection on the first true leaves of 5–9 individual plants (600–800 total penetration attempt counted per genotype). Different letters show statistical differences according to Tukey's post-hoc test following one-way ANOVA. There was a significant genotype effect in both Fig3A and Fig3D ($p<0.0001$). (B, E) Root length of 7-day-old seedlings grown in the presence or absence of cadmium (50 µM CdCl2, between 25-30 individual seedlings for each genotype/treatment grown on the same plate have been used for the measurement). Different letters show statistical differences within treatment groups according to Tukey's post-hoc test following two-way ANOVA. For both Fig3B and Fig3E there were significant main effects for Cd treatment and genotype ($p<0.001$), and a significant interaction effect ($p<0.001$). (C-F) Phytochelatin accumulation in 4-day-old seedlings transferred for two days on 50 µM CdCl2. Different letters show statistical differences within PC length groups according to Tukey's post-hoc test following two-way ANOVA. For both Fig3C and Fig3F, there were significant main effects for the genotype and the PC length factor ($p<0.001$), and a significant interaction effect ($p<0.001$).

the two functions of PCS1 in heavy metal tolerance and immunity can be uncoupled. This suggests that disease resistance conferred by PCS1 is independent of the ability of the enzyme to synthesize phytochelatin.

To test this hypothesis, we generated catalytically inactive PCS1 mutants to investigate the importance of phytochelatin production for fungal resistance. The phytochelatin synthase activity of PCS1 is dependent on a highly conserved catalytic triad located in the N-terminal half of the protein, consisting of Cys56, His162 and Asp180 (Romanyuk et al., 2006). Notably, the cysteine at position 56 has been shown to be involved in the formation of an acyl-enzyme intermediate (Vatamaniuk et al., 2004). Thus, PCS1 proteins carrying C56A, C56S or H162A substitutions lack PC synthesis activity *in vitro* (Vatamaniuk et al., 2004; Romanyuk et al., 2006). To test directly whether the function of PCS1 in fungal resistance is dependent on phytochelatin biosynthesis, we generated transgenic *pcs1pcs2* Arabidopsis plants expressing, under its native promoter, the genomic coding sequence of wild-type PCS1 ($PCS1_{WT}$) or constructs carrying either a C56S ($PCS1_{C56S}$) or H162A ($PCS1_{H162A}$) amino acid substitution in PCS1. As predicted by the inability of the mutated proteins to synthesize phytochelatin (PC) *in vitro* (Vatamaniuk et al., 2004; Romanyuk et al., 2006), transgenic lines expressing $PCS1_{C56S}$ or $PCS1_{H162A}$ were deficient in PC *in vivo* (Figure 3F) and showed the same degree of root growth inhibition as *pcs1pcs2* when grown on 50 µM cadmium chloride (Figure 3E). In contrast, in $PCS1_{C56S}$ or $PCS1_{H162A}$ lines, *Bgh* entry frequencies were similar to those seen in wild-type Col-0 plants or *pcs1pcs2* complemented by $PCS1_{WT}$ (Fig. 3D). These results confirm that the function of PCS1 in fungal resistance depends on a PCS1 activity or function that is distinct from phytochelatin synthesis.

PCS1, but not phytochelatin synthase activity, is involved in indole glucosinolate metabolism to restrict powdery mildew entry in Arabidopsis cells

As indicated by the aberrant accumulation of 4-methoxyindol-3-ylmethyl glucosinolate (4MI3G) and IG-metabolism products in *pcs1* plants upon flg22 or Cd^{2+} treatment, or inoculation with *P. infestans* (Clay et al., 2009; De Benedictis et al., 2018; Matern et al., 2019), PCS1, like PEN2, is required for the pathogen-inducible metabolism of IGs. Similarly, upon inoculation with *Bgh*, *pen2* and *pen4* hyperaccumulate 4MI3G (Fig .4B) and are not able to produce indol-3-ylmethylamine (I3A, Fig. 4C) and raphanusamic acid (RA, Fig. 4D). Levels of IGs and their metabolic products are restored to wild-type levels when the *pen4* or *pcs1pcs2* mutants are complemented by either GFP-PCS1 or the mutated $PCS1_{C56S}$ or $PCS1_{H162A}$, consistent with their wild-type-like disease resistance phenotype (Fig. 4B-D). The ABC transporter PEN3/PDR8/ABCG36, although not deficient in I3A or RA (Bednarek et al., 2009), is thought to be involved in this IG metabolic pathway as an exporter of pro-toxins or

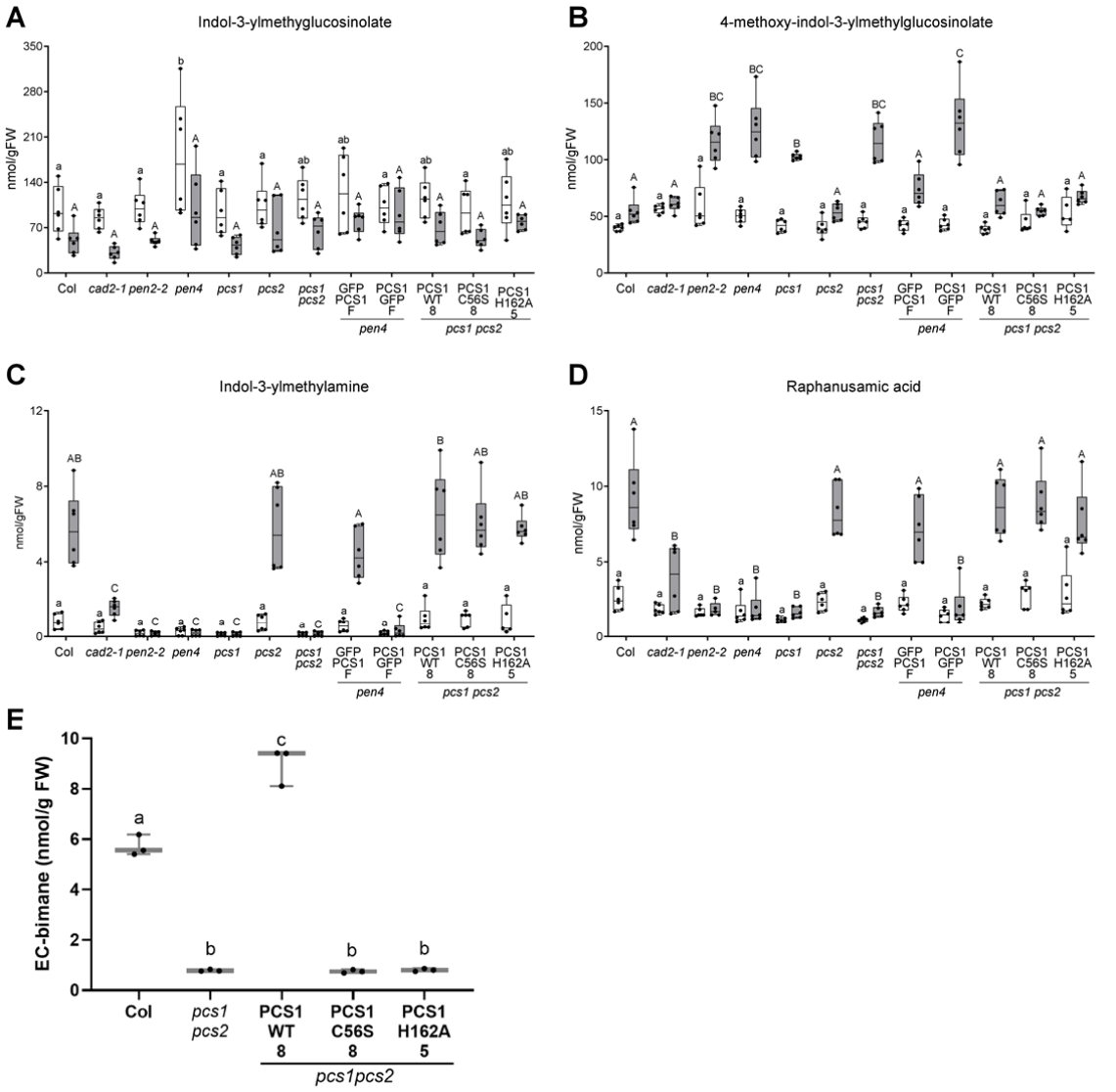

Figure 4. **PCS1 is involved in indole glucosinolate metabolism.**
(A-D) Box plots showing accumulation of selected secondary metabolites, indicated as nmol/g of fresh tissue weight (FW), in Arabidopsis genotypes 16 hours after inoculation with Bgh conidiospores (gray bars). (n=6). (A) Indol-3-ylmethylglucosinolate (I3G), (B) 4-methoxyindol-3-ylmethylglucosinolate (4MI3G), (C) Indol-3-ylmethylamine (I3A) (D) Raphanusamic acid (RA). Different letters show statistical differences according to Tukey's post-hoc test following two-way ANOVA. We observed significant main effects for Bgh inoculation and genotype ($p<0.0001$), and a significant interaction effect ($p<0.0001$) for 4MI3G, I3A and RA. In the case of I3G only significant main effects for Bgh inoculation and genotype ($p<0.0001$), but no interaction effect, were observed. (E) EC-bimane content in seedlings infiltrated with ECG-bimane measured by HPLC (n=3). Different letters show statistical differences according to Tukey's post-hoc test following one-way ANOVA. There was a significant genotype effect ($p<0.0001$).

304 toxic end products (Stein et al., 2006). This putative role would explain the proper
305 accumulation of I3A/RA and hyper-accumulation of 4-*O*-β-D-glucosyl-indol-3-yl formamide
306 (4OGlcI3F), a product presumably formed upon PEN2-mediated hydrolysis of 4MI3G, in
307 *pen3* leaves inoculated with *Bgh* (Lu et al., 2015). Our analysis of *pcs1* mutants revealed that
308 in addition to I3A and RA, PCS1 is also indispensable for 4OGlcI3F accumulation during the
309 Arabidopsis response to pathogen inoculation (Fig. S4A).
310
311 To directly test whether PEN2 and PEN4 operate in the same pathway, the two mutants were
312 crossed. The *pen2 pen4* double mutant supported a similar increase in entry frequency by *Bgh*

as did the *pen2* or *pen4* single mutants (Fig. S4B). Together with the colocalization with PEN2, these results suggest that PEN2 and PEN4 act together in one pathway that confers extracellular resistance to fungal attack. The correlation between the lack of pathogen-triggered accumulation of I3A and RA and defective entry resistance in *pcs1* lines emphasizes the importance of PCS1 in IG metabolism.

Upon pathogen challenge, the *pen4* mutant hyper-accumulates the physiological substrate of PEN2 myrosinase, 4MI3G, but not its unsubstituted precursor I3G (Figure 4A, B). In contrast, the pathogen-induced accumulation of both IG- and 4MI3G-derived hydrolysis products is essentially abolished (Fig. 4C, D, Fig. S4A). This phenocopies the metabolite profile seen in *pen2* plants (Bednarek et al., 2009; Lu et al., 2015), suggesting that like PEN2, PCS1 may act downstream of 4MI3G biosynthesis to produce I3A, RA and 4OGlcI3F, but upstream of the ABC transporter PEN3/PDR8.

Is PCS1 peptidase activity required for IG metabolism?

Phytochelatin synthases are known for their γ-glutamylcysteine dipeptidyl transpeptidase activity (EC 2.3.2.15), which catalyzes the transfer of the dipeptide glutamyl-cysteine (EC) from ECG onto another EC unit to generate the polypeptide phytochelatins $(EC)_n$-G. In addition, PCS has also been shown to be involved in the turnover of glutathione conjugates of xenobiotics by cleaving the glycine residue of their ECG moiety (Beck et al., 2003; Grzam et al., 2006; Blum et al., 2007).

It has been proposed that the IG-derived ITCs could be glutathionylated by GSTU13 and further processed by peptidases including PCS1 (Piślewska-Bednarek et al., 2018). To investigate whether the PC-deficient [*pen4*]-complementing mutants $PCS1_{C56S}$ and $PCS1_{H162A}$ still possessed peptidase activity, we assayed their deglycination activity on glutathionylated bimane (ECG-bimane, Blum et al. 2007). None of the PC-deficient lines could produce EC-bimane from ECG-bimane (Fig. 4E). This suggests that, unlike PCS1 metabolism of IG-derived compounds, both PC synthesis and the deglycination of glutathione conjugates depends on the residues C56 and H162 of the catalytic triad.

DISCUSSION

Phytochelatin synthase is primarily known for its role in tolerance of heavy metals, notably of cadmium (Grill et al., 1989; Clemens et al., 1999). Here, we identified PEN4/*At*PCS1 as a player in pre-invasive immune responses against fungal pathogens. The second PCS paralogue, the weakly expressed protein *At*PCS2, appears to be dispensable for both heavy metal tolerance and disease resistance. *pcs1* mutants are hypersusceptible to adapted and non-adapted fungi, unveiling the importance of PCS1 for defense against fungal invasion. This impaired pre-invasive immunity might also explain the previously reported strong cell death phenotype in Arabidopsis *pcs1* plants in response to inoculation with the non-adapted oomycete pathogen *P. infestans*, because invasive growth of this oomycete in *pen2* plants is also linked to a localized plant cell death response (Lipka et al., 2005; Kühnlenz et al., 2015). Like the other PEN proteins, PCS1 concentrates underneath the penetration site of fungal appressoria. Interestingly, in uninfected cells PCS1 is cytosolic, and in response to infection it relocalizes to an endomembrane compartment(s) at incipient entry sites of attack. We did not observe this aggregation phenomenon after cadmium treatment, further underlining the dual functions of PCS1. Colocalization of RFP-PCS1 and PEN2-GFP in plant cells under attack suggests that these compartments are mitochondria as previously reported (Fuchs et al., 2016). Recent proteome studies localized PCS1 to the cytosol (Ito et al., 2011) and to the Arabidopsis mitochondrial complexome (Senkler et al., 2017), supporting its dual localization capacity.

Unlike the *pen1 pen2* double mutant (Lipka et al., 2005), the susceptibility of the *pen2 pen4* mutant to fungal infection is not more pronounced than either of the single mutants (Fig.S4). This suggests that PEN2 and PEN4/PCS1 act in the same pathway. PEN2 has been shown to be an essential component of an IG metabolism pathway involved in broad-spectrum resistance against filamentous eukaryotic pathogens (Bednarek et al., 2009; Pastorczyk and Bednarek, 2016). PCS1 appears to be equally involved in this pathway as the *pcs1* mutants exhibit exactly the same I3A, RA and 4OGlcI3F deficiencies as *pen2* plants (Fig. 4A,B and S4A) (Matern et al., 2019). The co-localization of both enzymes in response to pathogen attack could facilitate stimulus-induced metabolite channeling of these metabolites, which in turn could account for the lack of detection of the intermediates between I3G and I3A/RA or 4MI3G and 4OGlcI3F. However, this does not allow us to unambiguously determine whether PEN4 acts upstream, or downstream, or in parallel to PEN2.

The shared phenotype of the *pen2* and *pen4* mutants and the colocalization of PEN2 and PEN4 in the same compartment at the site of fungal ingress suggested a possible protein-protein interaction. However, we did not obtain any positive interactions between PEN2 and PEN4 in split-ubiquitin yeast two-hybrid experiments (Fig S5A), nor could we co-immunoprecipitate these two proteins from infected leaves (Fig. S5B). The lack of physical interaction is confirmed by the fact that PCS1 is still able to relocalize in a null *pen2* mutant background (Fig. 2F and S3F). Focal accumulation of the PEN3 ABC transporter as disks in the plasma membrane and co-localization of PEN2 and PEN4 aggregates on mitochondria underneath pathogen contact sites rather points to pathogen-inducible macromolecular crowding as a potential alternative mechanism. Such an arrangement of PEN2 and PEN4 would facilitate metabolite channelling for targeted release of antimicrobials (Ellis, 2001; Stein et al., 2006; Fuchs et al., 2016; Guigas and Weiss, 2016). However, it remains to be tested whether enforced PEN4 mislocalization impairs its activity in extracellular defense.

Using mutated versions of PCS1, we showed that the function of PCS1 in IG metabolism does not require phytochelatin synthase activity *sensu stricto* as we could generate PC-deficient mutants functional for IG metabolism. Indeed, the ability to metabolize IGs is retained in mutant versions of PCS1 (Fig. 4A-D) that cannot produce any phytochelatins (fig.3F) nor cleave the ECG bimane conjugate (Fig. 4E). Our findings confirm and extend a previous study in which heterologous expression of *Caenorhabditis elegans PCS* in the Arabidopsis *psc1* background complemented cadmium hypersensitivity, but not a leaf cell death phenotype in response to *P. infestans* inoculation (Kühnlenz *et al.,* 2015). Residue Cys56 of the catalytic triad (Cys56, H162, Asp180) has been implicated in the formation of an acyl-enzyme intermediate with γ-EC. There appears to be an as yet unidentified second acylation site in the C-terminal part of PCS1, which shows a low level of sequence conservation across plant species (Vatamaniuk et al., 2004; Rea, 2012). This second site, which is absent in prokaryotic PCS, could potentially participate in IG metabolism. This hypothesis is supported by the fact that the PCS from *C. elegans* that was not able to complement the cell death phenotype in *pcs1* plants has a significantly shorter C-terminal part compared to *At*PCS1 (Rea et al., 2004; Kühnlenz et al., 2015). This assumed significance of the PCS1 C-terminus could also explain why GFP-PCS1, but not the PCS1-GFP fusion, is non-functional in IG metabolism and extracellular defense despite its proper subcellular localization. Alternatively,

413 rather than acting catalytically PCS1 may instead stabilize a chemically labile intermediate in
414 the IG metabolism pathway or stabilize a protein complex required for IG catabolism.
415
416 The chemical structures of RA and I3A, combined with the fact that their formation is
417 dependent on ECG supply via γ-glutamylcysteine synthetase, suggested indol-3-ylmethyl-
418 ITC-ECG conjugates as intermediates in pathogen-triggered IG metabolism in Brassicaceae
419 (Bednarek et al., 2009). The existence of such conjugates *in planta* is supported by the
420 identification of indolyl-dithiocarbamate glucoside during engineering of brassinin (an IG-
421 derived phytoalexin from *Brassica* spp.) biosynthesis in *Nicotiana benthamiana* (Klein and
422 Sattely, 2017). GSTU13 was recently found to be essential for pathogen-inducible formation
423 of RA, I3A, and 4OGlcI3F, suggesting that it catalyzes the conjugation of unstable
424 glucosinolate hydrolysis products, the indol-3-ylmethyl-ITCs, with ECG to form a
425 dithiocarbamate adduct *in planta* (Piślewska-Bednarek et al., 2018). Although the exact
426 mechanism of PCS1 in this pathway remains to be defined, our analysis combined with earlier
427 work (Matern et al. 2019) suggests PCS1 as a plausible candidate for further processing of
428 this adduct to I3A and RA, and the corresponding 4-methoxy adduct to 4OGlcI3F. However,
429 as mentioned above, we cannot exclude that PCS1 acts upstream of GSTU13, or even in
430 parallel to PEN2, or that it controls expression of the corresponding genes (Fig. 5). In
431 conclusion, AtPCS1 is a multi-functional protein: it detoxifies xenobiotics via chelation of
432 heavy metals by phytochelatin or via degradation of glutathione conjugates, and it participates
433 in the production of antimicrobials formed from IGs in the PEN2 pathway.
434
435 **MATERIALS AND METHODS**
436
437 **Plant and fungal lines and growth conditions**
438
439 *Arabidopsis thaliana* plants were grown for 15 to 20 days in growth chambers at 22°C with a
440 12-h photoperiod. All Arabidopsis mutants and transgenic lines were in the Columbia
441 background (Table S2). Host powdery mildew (*Golovinomyces cichoracearum* UCSC1) was
442 cultured on squash for 10 to 12 days and then applied to Arabidopsis using settling towers.
443 Non-host barley powdery mildew (*Blumeria graminis f. sp hordei* CR3) was grown on barley
444 (*Hordeum vulgare*) line Algerian-S (CI-16138) and inoculated onto Arabidopsis using the
445 methods described by Zimmerli et al. (2004).
446

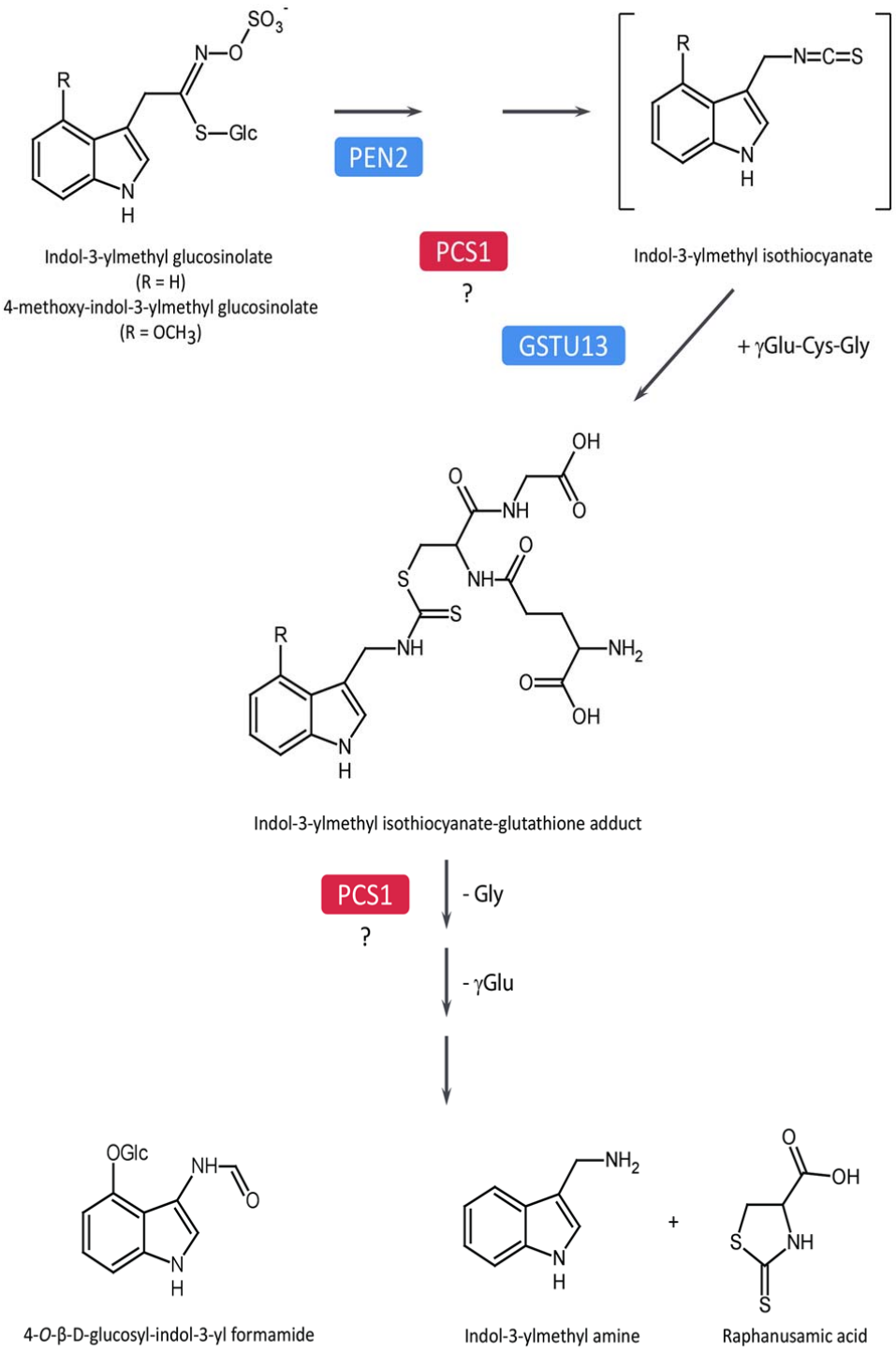

Figure 5. **Function of PCS1 in pathogen-triggered indole glucosinolate metabolism.**
As indicated by a deficiency in indole glucosinolate hydrolysis products and hyper-accumulation of 4-methoxy-indol-3-ylmethyl glucosinolate in pcs1 mutant plants, PCS1 acts downstream of intact glucosinolates. PCS1 might contribute to the processing of the isothiocyanate-glutathione adduct, modulate the activity of other enzymes of the pathway or control expression of the corresponding genes.

447 Transgenic Arabidopsis lines were generated according to the floral dip method (Clough and

448 Bent, 1998), T1 lines carrying single T-DNA insertion events were identified by screening
449 their progeny for segregation of antibiotic resistance in the appropriate ratio. Resistant T2
450 seedlings were transferred to soil and used in pathogen assays, in which several representative
451 independent lines were selected. T2 individuals homozygous for T-DNA insertions (based on
452 100% antibiotic resistance or 100% GFP fluorescence among their T3 progeny) were further
453 used for pathogen resistance or heavy metal tolerance assays and metabolic analysis.
454
455 For assaying tolerance to cadmium, Arabidopsis seeds were surface-sterilized and sown onto
456 agar plates containing half-strength Murashige and Skoog medium and 50 µM cadmium
457 chloride ($CdCl_2$). Plates were grown under continuous light at 22 °C. After seven days, plates
458 were scanned and root lengths measured from scanned images using the software ImageJ. All
459 experiments were repeated at least three times with similar results.
460
461 **Map-based cloning of PEN4**
462 The *pen4* mutation was mapped to the bottom arm of chromosome 5 using an F2 mapping
463 population generated from a cross between *pen4* and Landsberg-*erecta* (Ler), according to
464 Lukowitz et al. (2000). We narrowed down the region containing *PEN4* to a genomic interval
465 of approximately 20 kbp at the end of BAC clone MRH10. Analysis of lists of genes that co-
466 express with either *PEN1*, *PEN2* or *PEN3* across publicly available microarray datasets
467 (Obayashi et al., 2008) identified a gene highly correlated in expression with all three PEN
468 genes (Fig.S2) and that also resided in the 20 kbp mapping interval. Sequencing of this gene,
469 At5g44070, from the *pen4* mutant showed that it harbored a G to A transition at nucleotide
470 position 1,713 from the A of the translational start site of the genomic sequence. This
471 mutation results in a predicted truncation of the *At*PCS1 protein at residue 236.
472
473 **Plasmids and DNA constructs**
474 PCS1 fusions to GFP or RFP were constructed using Gateway technology (Invitrogen). The
475 Arabidopsis PCS1 (*At*PCS1) genomic coding sequence was amplified by PCR using BAC
476 clone MRH10 as template DNA and recombined into donor vector pDONR/Zeo (Invitrogen,
477 Table S1). The resulting entry vector was then recombined by a gateway LR reaction with the
478 destination vectors pMDC43 and pMDC83 (Curtis and Grossniklaus, 2003) to produce
479 expression clones GFP-PCS1 and PCS1-GFP, respectively. pDONR/Zeo *At*PCS1 was
480 recombined with a modified pEG106 (Gutierrez et al., 2009) containing an HA-tagged
481 mCherry to generate RFP-PCS1. GFP fusions were transformed into a *pen4* mutant

482 background (and selected on hygromycine 50 mg/L) and RFP-PCS1 into a *pcs1pcs2* double
483 mutant (Blum et al., 2007; selected on soil after BASTA spray). For complementation
484 analyses, the entire *PCS1* genomic coding sequence in addition to 3 kbp of promoter sequence
485 upstream of the translational start site and 1 kbp downstream of the translational stop codon
486 was amplified by PCR using BAC clone MRH10 as template DNA and recombined into
487 donor vector pDONR/Zeo. The QuikChange mutagenesis kit (Stratagene) was used to
488 introduce mutations in pDONR/Zeo $PCS1_{WT}$, resulting in a change of cysteine 56 to serine
489 ($PCS1_{C56S}$) or of histidine 162 to alanine ($PCS1_{H162A}$). The resulting entry vectors were then
490 recombined with destination vector pGWB1 (conferring resistance to hygromycin)
491 (Nakagawa et al., 2007) to generate expression clone PCS1-WT. These mutated PCS1
492 genomic clones were further recombined in the binary vector pGWB1. All expression clones
493 were introduced into *Agrobacterium tumefaciens* (strain GV3101), and the resulting strains
494 were used for stable transformation of Arabidopsis according to the floral dip method.
495
496 **Generation of double mutants**
497 Double mutants were generated by crossing the *pen4* mutant to *pen2-1*, *pen2-3* or *pen3-1*
498 mutants (Stein et al., 2006). F2 individuals homozygous at the mutated loci were identified
499 using the cleaved amplified polymorphic sequence (CAPS) markers described. For the CAPS
500 marker used to identify the *pen4* mutation, the *pen4* sequence was PCR-amplified with
501 forward primer 5'taagacaaaacttgtggattgg3' and reverse primer 5'cacccatctgatgaattgg3' and the
502 resulting DNA product was cleaved using the *Mbo*I restriction enzyme.
503
504 **Microscopic observations**
505 *Bgh* penetration assays were carried out as described by Zimmerli et al. (2004), and stained
506 with aniline blue according to Vogel and Somerville (2000). Successful penetrations
507 (resulting in haustoria with extensive callose encasement) and failed penetrations (resulting in
508 callosic papillae) were counted to determine the penetration rate (successful
509 penetration/number of attempts). For imaging of fluorescent proteins in Arabidopsis
510 epidermal cells, leaves from 2 to 3-week-old plants were mounted in a 0.01 mg/mL propidium
511 iodide solution in water (to stain fungal structures). Leaves were examined between 12 and 18
512 hours following fungal inoculation on a spinning disc confocal microscope consisting of a
513 Leica DMI 6000 B inverted microscope (Leica Microsystems, Wetzlar, Germany) fitted with
514 a Yokogawa CSU-10 spinning disc confocal attachment (Yokogawa Electric Corporation,
515 Tokyo, Japan) and a Photometrics QuantEM 512SC EM-CCD camera (Photometrics, Tucson,

AR). Samples were mounted in water and observed with a 63x water immersion objective. EGFP was excited at 488 nm, and fluorescence was collected through a 525/50 nm band-pass filter and fungal structures stained with propidium idodide at 620/60 band-pass filter (Chroma Technologies, Brattleboro, VT). RFP (mCherry) was excited at 561 nm, and fluorescence was collected through a 620/60 nm band-pass filter (Chroma Technologies, Brattleboro, VT). Microscope control and acquisition of images and z-series were accomplished using Metamorph software (Molecular Devices, Sunnyvale, CA), and image processing was performed by using ImageJ (W. Rasband, National Institutes of Health, Bethesda, MD) software.

Metabolic profiling

Analysis of phytochelatin biosynthesis and the bimane-conjugate hydrolysis assay were performed according to Blum et al. (2007). Extraction and analysis of indole glucosinolates and their derivatives were performed according to Bednarek et al. (2011) and Lu et al. (2015).

Statistical analysis

Statistical analysis was conducted with Graphpad Prism 8. Normality of samples was tested using D'Agostino & Pearson test ($p>0.05$). Normality was assumed for small size samples ($n<6$). ANOVA was performed coupled to a Tukey test in order to proceed to pairwise comparison between samples (confidence index, 95%). Statistical analyses between two samples were performed using the Student t-test (p-value=0.05). In the box plots the boxes indicate first and third quartile, the lines represent the median values, the whiskers indicate minimal and maximal values (excluding any outliers) and the points represent individual measurements.

ACKNOWLEDGEMENTS

We acknowledge the work of the late Ralph Blum for metabolite analysis and data processing shown in Figure 3C, F and Figure 4E.

We are grateful to Chris Cobbett (University of Melbourne, Australia) for providing the *cad1* mutants and to Phil Rea (University of Philadelphia, USA) for AtPCS1 cDNA; Ryan Guttierez (Carnegie Institution of Science, Stanford, USA) for the pEG106 mCherry vector; Chris Cobbett, Phil Rea and Stephan Clemens (IGB, Jena, Germany) for helpful discussions;

Bill Underwood (Energy Biosciences Institute, Berkeley, USA) for his advice and help in microscopy, Barbara Kracher for her help with statiscal analysis and the Somerville lab for stimulating discussion.

Financial support was provided by the National Science Foundation and the Carnegie Institution of Science (to SS), a Stanford Graduate Fellowship (to MS), the Max Planck Society (to PSL), by Deutsche Forschungsgemeinschaft (DFG) Research Grant SPP1212 (to PSL), DFG grant GR 938 (to EG) and DFG grant LI 1317/2-1 (to VL), by Spanish Ministry of Economy and Competitiveness (MINECO) grants BIO2015-64077-R and BIO2012-32910 (to AM) and the National Science Centre grant 2012/07/E/NZ2/04098 (to PB).

SHORT LEGENDS FOR SUPPLEMENTAL MATERIAL

Table S1. List of primers used in this study

Table S2. Mutant alleles used in this study

Fig. S1. *pen4* is allelic to *cad1*

Fig. S2. *pen4* is more susceptible to various fungal pathogens

Fig. S3: Upon pathogen attack, the functional fusion protein RFP-PCS1 translocates from the cytosol to the surface of immobilized mitochondria tagged with PEN2-GFP.

Fig. S4. PEN2 and PCS1 act in the same biochemical and immune pathways

Fig. S5. PCS1-PEN2 physical interaction assays.

FIGURE LEGENDS

Figure 1. PEN4/PCS1 is important for both non-host penetration resistance and heavy metal tolerance.

(A) Aniline blue-stained leaves of 3-week-old Arabidopsis plants 24 h after inoculation with *Bgh*. Aniline blue stains callose papillae symptomatic of failed penetration attempts, and callose-containing encasements of haustorial necks formed after a successful penetration by the fungal appressorium (red circles). **(B)** 7-day-old Arabidopsis seedlings of the indicated genotype grown in the presence or absence of cadmium (50 µM $CdCl_2$, between 25-30 individual seedlings for each genotype/treatment grown on the same plate have been used for the measurement). **(C)** Box plots showing penetration rate of *Bgh* spores on leaves of 3-week-

583 old Arabidopsis plants. Measurements were done 24 h post-infection on the first true leaves of
584 5–6 individual plants (600–800 total penetration attempts counted per genotype). Whiskers
585 represent Min-Max values. Different letters show statistical differences according to Tukey's
586 post-hoc test following one-way ANOVA There was a significant genotype effect ($p<0.0001$).
587 **(D)** Root length of 7-day-old seedlings grown in the presence or absence of cadmium (50 µM
588 $CdCl_2$, between 25-30 individual seedlings for each genotype/treatment grown on the same
589 plate have been used for the measurement). Different letters show statistical differences
590 according to Tukey's post-hoc test following two-way ANOVA. There were significant main
591 effects for Cd treatment and genotype ($p<0.001$) and a significant interaction effect ($p<0.001$).
592 **(E)** Domain organization of PCS1 showing the position of several mutant alleles (above) and
593 residues important for phytochelatin synthesis (below in red).

594

595 **Figure 2. Pathogen attack triggers translocation of cytoplasmic PCS1 and mitochondrial**
596 **colocalization with PEN2 at fungal penetration sites.**
597 3-week-old Arabidopsis seedlings were inoculated with the non-adapted powdery mildew
598 *Blumeria graminis sp. hordei* (*Bgh*). The epidermis of the first true leaves was visualized by
599 confocal laser scanning microscopy 12–16 h after *Bgh* inoculation. The fungal structures are
600 stained with propidium iodide except in GFP/RFP localization experiments. All pictures
601 represent averaged Z-projection of stacks of 30–50 sections, except in **(C)** where a single
602 median section is shown. Localization at the attempted penetration site of GFP-PCS1 **(A)** or
603 PCS1-GFP **(B)** in a *pen4* mutant leaf epidermal cell. **(C)** Cytosolic localization of soluble
604 GFP with RFP-PCS1 in non-infected epidermal cells. **(D)** Translocation of RFP-PCS1 but not
605 of soluble GFP into aggregates at the penetration site. **(E)** Colocalization of RFP-PCS1 with
606 mitochondria-associated PEN2-GFP at the penetration site. **(F)** Localization of GFP-PCS1 in
607 a *pen2* mutant background after *Bgh* infection. Scale bar is either 10 µm (A-C) or 5 µm (D-F).
608
609
610 **Figure 3: Phytochelatin synthesis is required for heavy metal tolerance but not for non-**
611 **host resistance.**
612 **(A, D)** Box plots showing penetration rate of *Bgh* spores on leaves of 3-week-old Arabidopsis
613 plants. Measurements were done 24 h post-infection on the first true leaves of 5–9 individual
614 plants (600–800 total penetration attempt counted per genotype). Different letters show
615 statistical differences according to Tukey's post-hoc test following one-way ANOVA. There

was a significant genotype effect in both Fig3A and Fig3D ($p<0.0001$). **(B, E)** Root length of 7-day-old seedlings grown in the presence or absence of cadmium (50 µM $CdCl_2$, between 25-30 individual seedlings for each genotype/treatment grown on the same plate have been used for the measurement). Different letters show statistical differences within treatment groups according to Tukey's post-hoc test following two-way ANOVA. For both Fig3B and Fig3E there were significant main effects for Cd treatment and genotype ($p<0.001$), and a significant interaction effect ($p<0.001$). **(C-F)** Phytochelatin accumulation in 4-day-old seedlings transferred for two days on 50 µM $CdCl_2$. Different letters show statistical differences within PC length groups according to Tukey's post-hoc test following two-way ANOVA. For both Fig3C and Fig3F, there were significant main effects for the genotype and the PC length factor ($p<0.001$), and a significant interaction effect ($p<0.001$).

Figure 4. PCS1 is involved in indole glucosinolate metabolism.

(A-D) Box plots showing accumulation of selected secondary metabolites, indicated as nmol/g of fresh tissue weight (FW), in Arabidopsis genotypes 16 hours after inoculation with *Bgh* conidiospores (gray bars). (n=6). **(A)** Indol-3-ylmethylglucosinolate (I3G), **(B)** 4-methoxyindol-3-ylmethylglucosinolate (4MI3G), **(C)** Indol-3-ylmethylamine (I3A) **(D)** Raphanusamic acid (RA). Different letters show statistical differences according to Tukey's post-hoc test following two-way ANOVA. We observed significant main effects for *Bgh* inoculation and genotype ($p<0.0001$), and a significant interaction effect ($p<0.0001$) for 4MI3G, I3A and RA. In the case of I3G only significant main effects for *Bgh* inoculation and genotype ($p<0.0001$), but no interaction effect, were observed. **(E)** EC-bimane content in seedlings infiltrated with ECG-bimane measured by HPLC (n=3). Different letters show statistical differences according to Tukey's post-hoc test following one-way ANOVA. There was a significant genotype effect ($p<0.0001$).

Figure 5. Function of PCS1 in pathogen-triggered indole glucosinolate metabolism.

As indicated by a deficiency in indole glucosinolate hydrolysis products and hyper-accumulation of 4-methoxy-indol-3-ylmethyl glucosinolate in *pcs1* mutant plants, PCS1 acts downstream of intact glucosinolates. PCS1 might contribute to the processing of the isothiocyanate-glutathione adduct, modulate the activity of other enzymes of the pathway or control expression of the corresponding genes.

Figure S1. *pen4* is allelic to *cad1/pcs1*.

Box plots showing penetration rate of *Bgh* sporelings on leaves of 3-week-old Arabidopsis plants. Measurements were carried out 24 h post *Bgh* spore inoculation on the first true leaves of 8 individual plants (>800 total penetrations attempt counted per genotype). *** $p<0.001$; * $p<0.05$ according to Student's t-test.

Figure S2. *pen4* is more susceptible to various fungal pathogens

Quantification of infection by *Plectosphaerella cucumerina* (**A**) or *Botrytis cinerea* (B, 7dpi) and the biotrophic mildew pathogen *Golovinomyces cichoracearum* (C, 7dpi). (**A**) Percentage of susceptible plants of the indicated genotypes at different days after inoculation (dpi) with 4×10^6 *P. cucumerina* spores/ml. Data represent the average (±SE, n>10) from one of three independent experiments that gave similar results. (**B**) Percentage of plant fresh weight (FW) reduction of the indicated genotypes at seven days after inoculation with 5×10^4 *B. cinerea* spores/ml. Data represent the average (±SE, n>10) of three independent experiments. (**C**) Pictures of first true leaves of 3 week-old Arabidopsis rosette inoculated with *Golovinomyces cichoracearum*.

Figure. S3: Upon pathogen attack, the functional fusion protein RFP-PCS1 translocates from the cytosol to the surface of immobilized mitochondria tagged with PEN2-GFP.

(**A-B**) RFP-PCS1 fusion complements *pcs1pcs2* mutant phenotypes. **(A**) Penetration rate of *Blumeria graminis* on *Arabidopsis thaliana* leaf epidermal cells. Box plots showing penetration rate of *Bgh* spores on leaves of 3-week-old Arabidopsis plants. Measurements were done 24 h post-infection on the first true leaves of 5 individual plants (600–800 total penetration attempts counted per genotype). Different letters show statistical differences according to Tukey's post-hoc test following one-way ANOVA. There was a significant genotype effect ($p<0.0001$). (**B**) 7-day-old Arabidopsis seedlings of the indicated genotype grown in the presence or absence of cadmium (50 µM $CdCl_2$, between 25-30 individual seedlings for each genotype/treatment grown on the same plate have been used for the measurement). Different letters show statistical differences within treatment groups according to Tukey's post-hoc test following two-way ANOVA. There was a significant main effect for Cd treatment and for the genotype factor ($p<0.001$), and a significant interaction effect ($p<0.001$). (C-E) Confocal images show unchallenged (**C**) and challenged (D, E) leaf epidermal cells of stable double transgenic plants transformed with P_{PEN2}::PEN2-GFP and

P_{35S}::RFP-PCS1 constructs. In unchallenged epidermal cells (**C**), RFP-PCS1 shows a cytoplasmic localization pattern, whereas PEN2-GFP can be detected in the cytoplasm and the periphery of mobile membrane compartments (recently demonstrated to represent mitochondria and peroxisomes). Pathogen challenge triggers co-localization patterns in aggregate structures with enhanced fluorescence intensity (**D,E**). Notably, in contrast to PEN2-GFP, RFP-PCS1 cannot be detected in the periphery of organelles (E, white arrows). 20 hpi with *Bgh*. (**F**) Transgenic *pen2-1* knockout lines expressing RFP-PCS1 show pathogen-induced aggregate formation in the absence of PEN2. 19 hpi with *Bgh.* White dotted line indicates position of the fungal appressorium. ap, appressorial germ tube. Bars = 10 μm.

Figure S4. PEN2 and PCS1 act in the same biochemical and immune pathways

(A) Accumulation of 4-*O*-β-D-glucosyl-indol-3-yl formamide, indicated as nmol/g of fresh tissue weight (FW), in different Arabidopsis genotypes 16 hours after inoculation with *Bgh* conidiospores. (n=9). Different letters show statistical differences according to Tukey's post-hoc test following two-way ANOVA. We observed significant main effects for Bgh inoculation and genotype ($p<0.0001$), and a significant interaction effect ($p<0.0001$). (B) penetration rate of *Blumeria graminis* on *Arabidopsis thaliana* leaf epidermal cells. Box plots showing penetration rate of *Bgh* spores on leaves of 3 week-old Arabidopsis plants. Measurements were done 24 h post-infection on the first true leaves of 6 individual plants (600–800 total penetration attempts counted per genotype). Different letters show statistical differences according to Tukey's post-hoc test following one-way ANOVA. There was a significant genotype effect ($p<0.0001$).

Figure. S5. PCS1-PEN2 physical interaction assays.

(**A**) Split-ubiquitin Y2H assays suggest no direct interaction of PEN2 and PCS1. Only yeast cells containing the positive control KAT1 grow on selective medium (-Ade, -His). (**B**) Co-immunoprecipitation experiments suggest that PEN2 and PCS1 do not interact with each other. 3-week-old plants expressing PEN2-GFP and 3xHA-RFP-PCS1 were infected (Inf) or not (UI). Total leaf protein extracts were subjected to a PEN2-immunoprecipitation (anti-GFP agarose beads) and purified fractions (B: bound, UB: unbound) were tested by western blotting against PEN2 (anti-GFP) and PCS1 (anti-HA).

Parsed Citations

Beck A, Lendzian K, Oven M, Christmann A, Grill E (2003) Phytochelatin synthase catalyzes key step in turnover of glutathione conjugates. Phytochemistry 62: 423-431
Pubmed: Author and Title
Google Scholar: Author Only Title Only Author and Title

Bednarek P, Pislewska-Bednarek M, Svatos A, Schneider B, Doubsky J, Mansurova M, Humphry M, Consonni C, Panstruga R, Sanchez-Vallet A, Molina A, Schulze-Lefert P (2009) A glucosinolate metabolism pathway in living plant cells mediates broad-spectrum antifungal defense. Science 323: 101-106
Pubmed: Author and Title
Google Scholar: Author Only Title Only Author and Title

Bednarek P, Piślewska-Bednarek M, Ver Loren van Themaat E, Maddula RK, Svatoš A, Schulze-Lefert P (2011) Conservation and clade-specific diversification of pathogen-inducible tryptophan and indole glucosinolate metabolism in Arabidopsis thaliana relatives. New Phytologist 192: 713-726
Pubmed: Author and Title
Google Scholar: Author Only Title Only Author and Title

Berens ML, Berry HM, Mine A, Argueso CT, Tsuda K (2017) Evolution of Hormone Signaling Networks in Plant Defense. Annual Review of Phytopathology 55: 401-425
Pubmed: Author and Title
Google Scholar: Author Only Title Only Author and Title

Berens ML, Wolinska KW, Spaepen S, Ziegler J, Nobori T, Nair A, Krüler V, Winkelmüller TM, Wang Y, Mine A, Becker D, Garrido-Oter R, Schulze-Lefert P, Tsuda K (2019) Balancing trade-offs between biotic and abiotic stress responses through leaf age-dependent variation in stress hormone cross-talk. Proceedings of the National Academy of Sciences 116: 2364-2373
Pubmed: Author and Title
Google Scholar: Author Only Title Only Author and Title

Blum R, Beck A, Korte A, Stengel A, Letzel T, Lendzian K, Grill E (2007) Function of phytochelatin synthase in catabolism of glutathione-conjugates. Plant Journal 49: 740-749
Pubmed: Author and Title
Google Scholar: Author Only Title Only Author and Title

Blum R, Meyer KC, Wünschmann J, Lendzian KJ, Grill E (2010) Cytosolic Action of Phytochelatin Synthase. Plant Physiology 153: 159-169
Pubmed: Author and Title
Google Scholar: Author Only Title Only Author and Title

Clay NK, Adio AM, Denoux C, Jander G, Ausubel FM (2009) Glucosinolate metabolites required for an Arabidopsis innate immune response. Science 323: 95-101
Pubmed: Author and Title
Google Scholar: Author Only Title Only Author and Title

Clemens S, Kim EJ, Neumann D, Schroeder JI (1999) Tolerance to toxic metals by a gene family of phytochelatin synthases from plants and yeast. EMBO Journal 18: 3325-3333
Pubmed: Author and Title
Google Scholar: Author Only Title Only Author and Title

Clough SJ, Bent AF (1998) Floral dip: a simplified method for Agrobacterium-mediated transformation of Arabidopsis thaliana. The Plant Journal 16: 735-743
Pubmed: Author and Title
Google Scholar: Author Only Title Only Author and Title

Cobbett C, Goldsbrough P (2002) PHYTOCHELATINS AND METALLOTHIONEINS: Roles in Heavy Metal Detoxification and Homeostasis. Annual Review of Plant Biology 53: 159-182
Pubmed: Author and Title
Google Scholar: Author Only Title Only Author and Title

Collins NC, Thordal-Christensen H, Lipka V, Bau S, Kombrink E, Qiu JL, Huckelhoven R, Stein M, Freialdenhoven A, Somerville SC, Schulze-Lefert P (2003) SNARE-protein-mediated disease resistance at the plant cell wall. Nature 425: 973-977
Pubmed: Author and Title
Google Scholar: Author Only Title Only Author and Title

Curtis MD, Grossniklaus U (2003) A Gateway Cloning Vector Set for High-Throughput Functional Analysis of Genes in Planta. Plant Physiology 133: 462-469
Pubmed: Author and Title
Google Scholar: Author Only Title Only Author and Title

Cutler SR, Ehrhardt DW, Griffitts JS, Somerville CR (2000) Random GFP::cDNA fusions enable visualization of subcellular structures in cells of Arabidopsis at a high frequency. Proceedings of the National Academy of Sciences 97: 3718-3723
Pubmed: Author and Title
Google Scholar: Author Only Title Only Author and Title

Czerniawski P, Bednarek P (2018) Glutathione S-Transferases in the Biosynthesis of Sulfur-Containing Secondary Metabolites in Brassicaceae Plants. Frontiers in Plant Science 9: 1639
Pubmed: Author and Title
Google Scholar: Author Only Title Only Author and Title

De Benedictis M, Brunetti C, Brauer EK, Andreucci A, Popescu SC, Commisso M, Guzzo F, Sofo A, Ruffini Castiglione M, Vatamaniuk OK, Sanità di Toppi L (2018) The Arabidopsis thaliana Knockout Mutant for Phytochelatin Synthase1 (cad1-3) Is Defective in Callose Deposition, Bacterial Pathogen Defense and Auxin Content, But Shows an Increased Stem Lignification. Frontiers in Plant Science 9: 19
Pubmed: Author and Title
Google Scholar: Author Only Title Only Author and Title

Ellis RJ (2001) Macromolecular crowding: obvious but underappreciated. Trends in Biochemical Sciences 26: 597-604
Pubmed: Author and Title
Google Scholar: Author Only Title Only Author and Title

Fuchs R, Kopischke M, Klapprodt C, Hause G, Meyer AJ, Schwarzländer M, Fricker MD, Lipka V (2016) Immobilized subpopulations of leaf epidermal mitochondria mediate PENETRATION2-dependent pathogen entry control in Arabidopsis. Plant Cell 28: 130-145
Pubmed: Author and Title
Google Scholar: Author Only Title Only Author and Title

Grill E, Loffler S, Winnacker EL, Zenk MH (1989) Phytochelatins, the heavy-metal-binding peptides of plants, are synthesized from glutathione by a specific gamma-glutamylcysteine dipeptidyl transpeptidase (phytochelatin synthase). Proceedings of the National Academy of Sciences 86: 6838-6842
Pubmed: Author and Title
Google Scholar: Author Only Title Only Author and Title

Grill E, Winnacker EL, Zenk MH (1985) Phytochelatins: The Principal Heavy-Metal Complexing Peptides of Higher Plants. Science 230: 674-676
Pubmed: Author and Title
Google Scholar: Author Only Title Only Author and Title

Grzam A, Tennstedt P, Clemens S, Hell R, Meyer AJ (2006) Vacuolar sequestration of glutathione S-conjugates outcompetes a possible degradation of the glutathione moiety by phytochelatin synthase. FEBS Letters 580: 6384-6390
Pubmed: Author and Title
Google Scholar: Author Only Title Only Author and Title

Guigas G, Weiss M (2016) Effects of protein crowding on membrane systems. Biochimica et Biophysica Acta (BBA) - Biomembranes 1858: 2441-2450
Pubmed: Author and Title
Google Scholar: Author Only Title Only Author and Title

Gutierrez R, Lindeboom JJ, Paredez AR, Emons AMC, Ehrhardt DW (2009) Arabidopsis cortical microtubules position cellulose synthase delivery to the plasma membrane and interact with cellulose synthase trafficking compartments. Nature Cell Biology 11: 797
Pubmed: Author and Title
Google Scholar: Author Only Title Only Author and Title

Hematy K, Cherk C, Somerville S (2009) Host-pathogen warfare at the plant cell wall. Current Opinion in Plant Biology 12: 406-413
Pubmed: Author and Title
Google Scholar: Author Only Title Only Author and Title

Howden R, Goldsbrough PB, Andersen CR, Cobbett CS (1995) Cadmium-sensitive, cad1 mutants of Arabidopsis thaliana are phytochelatin deficient. Plant Physiology 107: 1059-1066
Pubmed: Author and Title
Google Scholar: Author Only Title Only Author and Title

Ito J, Batth TS, Petzold CJ, Redding-Johanson AM, Mukhopadhyay A, Verboom R, Meyer EH, Millar AH, Heazlewood JL (2011) Analysis of the Arabidopsis Cytosolic Proteome Highlights Subcellular Partitioning of Central Plant Metabolism. Journal of Proteome Research 10: 1571-1582
Pubmed: Author and Title
Google Scholar: Author Only Title Only Author and Title

Klein AP, Sattely ES (2017) Biosynthesis of cabbage phytoalexins from indole glucosinolate. Proceedings of the National Academy of Sciences 114: 1910-1915
Pubmed: Author and Title
Google Scholar: Author Only Title Only Author and Title

Koh S, Andre A, Edwards H, Ehrhardt D, Somerville S (2005) Arabidopsis thaliana subcellular responses to compatible Erysiphe cichoracearum infections. Plant Journal 44: 516-529
Pubmed: Author and Title
Google Scholar: Author Only Title Only Author and Title

Kühnlenz T, Westphal L, Schmidt H, Scheel D, Clemens S (2015) Expression of Caenorhabditis elegans PCS in the AtPCS1-deficient

Arabidopsis thaliana cad1-3 mutant separates the metal tolerance and non-host resistance functions of phytochelatin synthases. Plant, Cell & Environment 38: 2239-2247
Pubmed: Author and Title
Google Scholar: Author Only Title Only Author and Title

Lipka U, Fuchs R, Lipka V (2008) Arabidopsis non-host resistance to powdery mildews. Current Opinion in Plant Biology 11: 404-411
Pubmed: Author and Title
Google Scholar: Author Only Title Only Author and Title

Lipka V, Dittgen J, Bednarek P, Bhat R, Wiermer M, Stein M, Landtag J, Brandt W, Rosahl S, Scheel D, Llorente F, Molina A, Parker J, Somerville S, Schulze-Lefert P (2005) Pre- and postinvasion defenses both contribute to nonhost resistance in Arabidopsis. Science 310: 1180-1183
Pubmed: Author and Title
Google Scholar: Author Only Title Only Author and Title

Lu X, Dittgen J, Piślewska-Bednarek M, Molina A, Schneider B, Svatoš A, Doubský J, Schneeberger K, Weigel D, Bednarek P, Schulze-Lefert P (2015) Mutant Allele-Specific Uncoupling of PENETRATION3 Functions Reveals Engagement of the ATP-Binding Cassette Transporter in Distinct Tryptophan Metabolic Pathways. Plant Physiology 168: 814-827
Pubmed: Author and Title
Google Scholar: Author Only Title Only Author and Title

Lukowitz W, Gillmor CS, Scheible W-R (2000) Positional Cloning in Arabidopsis. Why It Feels Good to Have a Genome Initiative Working for You. Plant Physiology 123: 795-806
Pubmed: Author and Title
Google Scholar: Author Only Title Only Author and Title

Matern A, Böttcher C, Eschen-Lippold L, Westermann B, Smolka U, Döll S, Trempel F, Aryal B, Scheel D, Geisler M, Rosahl S (2019) A substrate of the ABC transporter PEN3 stimulates bacterial flagellin (flg22)-induced callose deposition in Arabidopsis thaliana. Journal of Biological Chemistry 294: 6857-6870
Pubmed: Author and Title
Google Scholar: Author Only Title Only Author and Title

Nakagawa T, Kurose T, Hino T, Tanaka K, Kawamukai M, Niwa Y, Toyooka K, Matsuoka K, Jinbo T, Kimura T (2007) Development of series of gateway binary vectors, pGWBs, for realizing efficient construction of fusion genes for plant transformation. J Biosci Bioeng 104: 34-41
Pubmed: Author and Title
Google Scholar: Author Only Title Only Author and Title

Obayashi T, Hayashi S, Saeki M, Ohta H, Kinoshita K (2008) ATTED-II provides coexpressed gene networks for Arabidopsis. Nucleic Acids Research 37: D987-D991
Pubmed: Author and Title
Google Scholar: Author Only Title Only Author and Title

Pastorczyk M, Bednarek P (2016) The function of glucosinolates and related metabolites in plant innate immunity. In S Kopriva, ed, Glucosinolates. Academic Press Ltd-Elsevier Science Ltd, London, pp 171-198
Pubmed: Author and Title
Google Scholar: Author Only Title Only Author and Title

Piślewska-Bednarek M, Nakano RT, Hiruma K, Pastorczyk M, Sanchez-Vallet A, Singkaravanit-Ogawa S, Ciesiołka D, Takano Y, Molina A, Schulze-Lefert P, Bednarek P (2018) Glutathione Transferase U13 Functions in Pathogen-Triggered Glucosinolate Metabolism. Plant Physiology 176: 538-551
Pubmed: Author and Title
Google Scholar: Author Only Title Only Author and Title

Rea PA (2006) Phytochelatin synthase, papain's cousin, in stereo. Proceedings of the National Academy of Sciences of the United States of America 103: 507-508
Pubmed: Author and Title
Google Scholar: Author Only Title Only Author and Title

Rea PA (2012) Phytochelatin synthase: of a protease a peptide polymerase made. Physiologia Plantarum 145: 154-164
Pubmed: Author and Title
Google Scholar: Author Only Title Only Author and Title

Rea PA, Vatamaniuk OK, Rigden DJ (2004) Weeds, worms, and more. Papain's long-lost cousin, phytochelatin synthase. Plant Physiology 136: 2463-2474
Pubmed: Author and Title
Google Scholar: Author Only Title Only Author and Title

Romanyuk ND, Rigden DJ, Vatamaniuk OK, Lang A, Cahoon RE, Jez JM, Rea PA (2006) Mutagenic definition of a papain-like catalytic triad, sufficiency of the N-terminal domain for single-site core catalytic enzyme acylation, and C-terminal domain for augmentative metal activation of a eukaryotic phytochelatin synthase. Plant Physiology 141: 858-869
Pubmed: Author and Title
Google Scholar: Author Only Title Only Author and Title

Sanchez-Rodriguez C, Estevez JM, Llorente F, Hernandez-Blanco C, Jorda L, Pagan I, Berrocal M, Marco Y, Somerville S, Molina A (2009) The ERECTA Receptor-Like Kinase Regulates Cell Wall-Mediated Resistance to Pathogens in Arabidopsis thaliana. Molecular Plant-Microbe Interactions 22: 953-963
Pubmed: Author and Title
Google Scholar: Author Only Title Only Author and Title

Senkler J, Senkler M, Eubel H, Hildebrandt T, Lengwenus C, Schertl P, Schwarzländer M, Wagner S, Wittig I, Braun H-P (2017) The mitochondrial complexome of Arabidopsis thaliana. The Plant Journal 89: 1079-1092
Pubmed: Author and Title
Google Scholar: Author Only Title Only Author and Title

Stein M, Dittgen J, Sanchez-Rodriguez C, Hou BH, Molina A, Schulze-Lefert P, Lipka V, Somerville S (2006) Arabidopsis PEN3/PDR8, an ATP binding cassette transporter, contributes to nonhost resistance to inappropriate pathogens that enter by direct penetration. Plant Cell 18: 731-746
Pubmed: Author and Title
Google Scholar: Author Only Title Only Author and Title

Underwood W, Somerville SC (2008) Focal accumulation of defences at sites of fungal pathogen attack. Journal of Experimantal Botany 59: 3501-3508
Pubmed: Author and Title
Google Scholar: Author Only Title Only Author and Title

Vatamaniuk OK, Mari S, Lang A, Chalasani S, Demkiv LO, Rea PA (2004) Phytochelatin synthase, a dipeptidyltransferase that undergoes multisite acylation with gamma-glutamylcysteine during catalysis: stoichiometric and site-directed mutagenic analysis of Arabidopsis thaliana PCS1-catalyzed phytochelatin synthesis. Journal of Biological Chemistry 279: 22449-22460
Pubmed: Author and Title
Google Scholar: Author Only Title Only Author and Title

Vogel J, Somerville S (2000) Isolation and characterization of powdery mildew-resistant Arabidopsis mutants. Proceedings of the National Academy of Sciences 97: 1897-1902
Pubmed: Author and Title
Google Scholar: Author Only Title Only Author and Title

Zimmerli L, Stein M, Lipka V, Schulze-Lefert P, Somerville S (2004) Host and non-host pathogens elicit different jasmonate/ethylene responses in Arabidopsis. The Plant Journal 40: 633-646
Pubmed: Author and Title
Google Scholar: Author Only Title Only Author and Title